Journal of Membrane Science 479 (2015) 246–255

Contents lists available at ScienceDirect

Journal of Membrane Science

journal homepage: www.elsevier.com/locate/memsci

PdCuAu ternary alloy membranes: Hydrogen permeation properties in the presence of H_2S

Ana M. Tarditi [a,*], Carolina Imhoff [a], Fernando Braun [a], James B. Miller [b,c], Andrew J. Gellman [b,c], Laura Cornaglia [a]

[a] Instituto de Investigaciones en Catálisis y Petroquímica (FIQ, UNL-CONICET), Santiago del Estero 2829, 3000 Santa Fe, Argentina
[b] Department of Chemical Engineering, Carnegie Mellon University, Pittsburgh, PA 15213, United States
[c] National Energy Technology Laboratory, US Department of Energy, Pittsburgh, PA 15262, United States

ARTICLE INFO

Article history:
Received 16 October 2014
Received in revised form
19 December 2014
Accepted 21 December 2014
Available online 30 December 2014

Keywords:
PdCuAu ternary alloy
Hydrogen separation
Sulfur tolerance

ABSTRACT

PdCuAu ternary alloy membranes with different component compositions were synthesized by sequential electroless deposition of components onto porous stainless steel substrates. The ternary with the highest Au content, $Pd_{69}Cu_{14}Au_{17}$, exhibited the highest hydrogen permeation flux, comparable to that of a $Pd_{91}Au_9$ membrane. Upon exposure to 100 ppm H_2S/H_2 at 673 K for 24 h, all PdCuAu membranes experienced flux reductions of ~55%, followed by recovery to ~80% of the initial hydrogen flux upon reintroduction of pure hydrogen at 400 °C. Complete flux recovery after H_2S exposure required hydrogen treatment at 500 °C. X-ray diffraction (XRD) analysis of the H_2S-exposed PdCuAu membranes revealed fcc alloy structure with no evidence of bulk sulfide formation. In agreement with the XRD results, sulfur was not detected in the bulk of H_2S-exposed samples by energy dispersive spectroscopy (EDS). However, analysis of H_2S-exposed PdCuAu alloys by X-ray photoelectron spectroscopy (XPS) depth profiling revealed low, but measureable, amounts of sulfur in the near-surface region, about 10 nm in depth. The depth profiles of samples after hydrogen recovery treatment showed significantly reduced sulfur content. These results indicate that H_2S exposure causes flux loss in PdCuAu alloys through a surface-poisoning mechanism, and that the surface sulfide can be removed—and flux recovered—by high temperature treatment in hydrogen.

1. Introduction

Hydrogen can be produced from several sources including fossil fuels and biomass for use as an alternative energy carrier. One especially promising technology for hydrogen production is the membrane reactor (MR), in which chemical reactions and product purification occur simultaneously. High efficiency, cost reduction and flexibility of operation can be achieved by using a hydrogen-selective membrane to extract hydrogen from the reactor during the reaction [1,2]. It is well known that Pd-based membranes are suitable for MR applications because of their highly hydrogen selective permeability [3].

Despite its high permeability, the implementation of pure Pd membranes is limited by embrittlement in the presence of H_2 at temperatures <573 K [4] and by membrane poisoning with contaminants such as CO and H_2S that are commonly present in coal-derived syngas [5–7]. Alloying Pd with minor components, such as Ag, Au and Cu, can enhance permeability and, at the same time, improve mechanical and chemical properties [8]. It is well known that binary alloys such as PdAu, PdCu and PdPt are more resistant than pure Pd to poisoning by contaminants such as H_2S and CO [9–11]. PdCu alloys have been extensively studied both experimentally and theoretically, not only because they do not exhibit low temperature hydrogen embrittlement, but also because, PdCu alloys with face-centered-cubic (fcc) structure are more resistant to H_2S poisoning than pure Pd. It has been reported that fcc PdCu alloys experience only a 20% hydrogen permeance decline when exposed to 20 ppm H_2S at 593 K, while an alloy composition in the body-centered-cubic phase (bcc) exhibited a decrease of about 90% under the same exposure conditions [12]. At lower temperatures (<673 K) Morreale et al. [13] reported a complete loss of permeability for bcc PdCu alloys [13].

Even though most reports have focused on PdCu for improving membrane sulfur resistance, the PdAu alloy is also receiving increasing attention [10]. A reduction of ~10% in the hydrogen flux for a $Pd_{60}Au_{40}$ foil but 95% for a $Pd_{60}Cu_{40}$ alloy was reported by McKinley [14] in the presence of 4.5 ppm H_2S at 623 K. At lower concentrations ($Pd_{95}Au_5$), Au prevents bulk sulfidation and

* Corresponding author. Tel.: +54 342 4536861.
E-mail address: atarditi@fiq.unl.edu.ar (A.M. Tarditi).

http://dx.doi.org/10.1016/j.memsci.2014.12.030
0376-7388/

preserves the permeability of electroless deposited PdAu membranes in H_2S/H_2 mixtures [10]. Gade et al. reported permeabilities for PdAu membranes with a range of compositions prepared by magnetron sputter followed by cold working [15]. In 20–50 ppm H_2S/H_2 at 673 K they observed a decrease in permeation inhibition as the Au content increased from 7% to 20%. The authors noted a strong dependence on the membrane fabrication technique of the lifetime in H_2S streams [15].

In the last few years, ternary alloys have been studied in an attempt to improve both hydrogen permeation properties and the poison tolerance of Pd-based membranes [16–18]. We previously reported the high H_2S tolerance of PdAgAu membranes synthesized by electroless deposition [18]. The membranes did not undergo bulk sulfide corrosion even after exposure to 1000 ppm H_2S/H_2 at 623 K [19]. Bredesen and coworkers [17] reported H_2S resistance of several PdAgTM (TM: Mo, Y, Au or Cu) ternary alloy membranes synthesized by magnetron sputtering. The best performance was obtained with a $Pd_{75}Ag_{22}Au_3$ membrane, which exhibited the smallest permeance loss and the lowest post-exposure surface sulfur content. For $Pd_{80}Au_{10}Pt_{10}$ alloy membranes synthesized by magnetron sputtering, a flux reduction of ~21% was reported when 20 ppm H_2S was added to a water–gas shift mixture at 673 K [16]. Recently, Way and coworkers [20] tested the effect of H_2S on hydrogen permeation through a $Pd_{74}Au_{12}Ag_{14}$ membrane prepared by sequential electroless deposition. Under exposure to a 20 ppm H_2S in H_2 stream, the H_2 permeance of the membrane was reduced by 52%, 60% and 75% at temperatures of 773 K, 723 K and 673 K, respectively, with respect to the permeance in pure H_2 [20]. From the data reported in the literature, it has been shown that Au-containing ternary alloys have the higher tolerance to sulfur poisoning.

A few studies have been published on the hydrogen permeation properties of PdCuAu ternary alloy membranes [21]. Moreover, no sulfur tolerance data for this alloy are unavailable to date. Peters et al. [22] reported a hydrogen permeability of $Pd_{70}Cu_{26}Au_4$ that was 2.5–5 times higher than that of a PdCu binary alloy with a similar Pd content. For the fcc PdCuAu system, Coulter et al. [21,22] found that hydrogen permeability decreases significantly with increasing Cu content, while the effect of Au is much smaller. We recently reported our characterization of the surfaces of PdCuAu ternary alloy samples that we prepared on porous stainless steel disks by sequential electroless deposition [23]. Alloy composition selections were guided by high-throughput studies of sulfur-uptake conducted at Carnegie Mellon University on composition spread alloy film (CSAF) combinatorial libraries [24]. Annealed CSAFs were exposed to 100 ppm H_2/H_2S at 673 K for 24 h and then characterized for S uptake by X-ray photoelectron spectroscopy (XPS) and energy dispersive spectroscopy (EDS). Alloy compositions for electroless deposition onto the porous steel disks were chosen from CSAF regions that displayed low S uptake, and therefore have high potential for corrosion resistance. XPS analysis of clean PdCuAu alloys revealed that the near-surface regions became enriched in Pd with respect to the bulk composition determined by EDS. In contrast, Low Energy Ion Scattering Spectroscopy (LEIS) and angle-resolved XPS (ARXPS) analyses showed that the top-most surface layers in all samples were Cu-rich compared with the bulk composition [23].

With the aim of characterizing the impact of H_2S exposure on the hydrogen permeability of the PdCuAu ternary alloys, several membranes were synthesized by sequential electroless deposition. The effect of H_2S was characterized by feeding a 100 ppm H_2S/H_2 stream over the stainless steel disk followed by a flux recovery stage in pure H_2. An XPS depth profile analysis was performed to determine the surface sulfur concentration after both H_2S exposure and hydrogen recovery.

2. Experimental

2.1. Membrane preparation

The PdCuAu alloy membranes studied were deposited on porous stainless steel discs (PSSD, 1.27 cm in diameter and of 4 mm thick, 0.1 μm grade). The PSSD supports were purchased from Mott Metallurgical Corporation®. Prior to any plating experiment, the supports were cleaned in a basic solution consisting of 0.12 M Na_3PO_4, 12 M H_2O, 0.6 M Na_2CO_3 and 1.12 M NaOH [25]. After that, the discs were oxidized at 773 K for 12 h. In order to avoid intermetallic diffusion between the stainless steel elements and the PdCuAu ternary alloy, the supports were first modified with ZrO_2 using the dip coating vacuum assisted method [26]. Solutions for activation of the substrate were prepared using acidulated solutions of $SnCl_2$ and $PdCl_2$. The chemical compositions of the plating solutions used are summarized in Table 1. The activation procedure consisted of first dipping the PSSD substrate in the $SnCl_2$ solution and then in the $PdCl_2$ solution with water rinsing between the immersions. After dipping the support in the palladium chloride solution it was rinsed with a 0.01 M HCl solution to avoid the re-oxidation of palladium. This cycle was repeated as needed, normally 3 times. The electroless plating technique was used to coat the support with a continuous metallic film. Palladium, gold and copper were deposited by sequential electroless deposition. In all membranes, palladium was deposited in two steps of 60 min each, followed by Au deposition. After the Pd and Au depositions, the samples were rinsed with water and dried at 393 K overnight. The Cu plating was performed on top of the Pd–Au layers, after activation with $SnCl_2$ and $PdCl_2$. The deposition of Pd onto a Cu surface was found to be difficult because Cu on the surface partially dissolves in the Pd plating bath [27]. Therefore, the first metal layer applied to the support was always Pd, then Au and finally a Cu layer was applied onto the Pd–Au layers. Plating times for Pd, Au and Cu were adjusted to achieve the desired metal composition in all cases. After the electroless deposition of Cu, the samples were immediately immersed in 0.01 M HCl to neutralize any residual plating solution, followed by rinsing with de-ionized water and ethanol to facilitate drying and preventing the oxidation of the copper layer. The sample was then heated to 773 K in H_2 atmosphere in order to form a homogeneous Pd–Au–Cu alloy by thermal diffusion. The desired composition of the samples was achieved by modification of the Au and Cu deposition times while maintaining the same Pd deposition time. The thickness of each PdAuCu layer was ~4 μm. To obtain a defect-free film a second set of Pd, Au and Cu layers was applied followed by a second heat treatment at to 773 K in H_2. The

Table 1
Chemical composition of Pd, Au and Cu electroless plating solutions and plating conditions.

	Pd	Au	Cu
$PdCl_2$ (g/L)	3.6	–	–
$AuCl_3 \cdot HCl \cdot 4H_2O$ (mmol/L)	–	7.5	–
$CuSO_4 \cdot 5H_2O$ (g/L)	–	–	20
NH_4OH (mL/L)	650	–	–
$Na_2EDTA \cdot 2H_2O$ (g/L)	67	–	30
N_2H_4 1 M (mL/L)	10	–	–
HCHO (37%) (mL/L)	–	–	14
NaOH (g/L)	–	7.2	20
EDA (ppm)	–	–	100
$K_4Fe(CN)_6 \cdot 3H_2O$ (ppm)	–	–	35
$(C_2H_5)_2NCS_2Na \cdot 3H_2O$ (ppm)	–	–	5
Na_2SO_3 (mol/L)	–	0.17	–
$Na_2S_2O_3 \cdot 5H_2O$ (mol/L)	–	0.15	–
L-$C_6H_8O_6$ (mol/L)	–	0.36	–
pH	11	11	12
Temperature (K)	323	333	298

nomenclature adopted for the samples was $Pd_xCu_yAu_{100-x-y}$ where x and y refer to the atomic bulk composition determined by EDS. The thickness of the metal layers was determined by the gravimetric method, in all cases being $\sim$14 μm.

2.2. Sample characterization

2.2.1. X-ray diffraction

The phase structure of the samples as a function of annealing time was determined by X-ray diffraction (XRD). The XRD patterns of the films were obtained with an XD-D1 Shimadzu instrument, using Cu Kα (λ=1.542 Å) radiation at 30 kV and 40 mA. The scan rate was 1–2° min^{-1} in the range 2θ=15–90°.

2.2.2. Scanning electron microscopy and energy-dispersive X-ray analysis

The outer surface and cross-section images of the samples were obtained using a JEOL scanning electron microscope (SEM), model JSM-35C, equipped with an energy dispersive analytical system (EDS).

2.2.3. XPS-depth profile experiments

XPS depth profiles were performed using a ThermoFisher Theta Probe instrument. The instrument has a base working pressure of 1.0×10^{-10} kPa; it is equipped with a monochromatic Al Kα X-ray source. A hemispherical analyzer was operated in constant analyzer energy mode with a pass energy of 200 eV. The depth profiles were performed using argon ion sputtering. A differentially pumped ion gun was operated at 1×10^{-8} kPa, 3 kV and 500 nA, conditions which delivered a sputtering rate of approximately 1 nm min^{-1}. Sputtering was performed in 10 steps of 30 s, followed by 10 steps of 90 s to examine the top $\sim$20 nm of the sample surfaces. Before sputtering and then at each sputtering step, XP spectra for Pd 3d, Pd 3p, O 1s, C 1s, Au 4f, Cu 2p, S 1s, S 2p core levels were recorded; peak areas were determined by integration employing a Shirley-type background. Sensitivity factors provided by the manufacturer were used for quantification of the elemental composition.

2.3. Hydrogen permeation measurements and H_2S treatment

Hydrogen single gas permeation experiments for membranes were conducted using the permeation module previously described [27]. In this case, the sealing was achieved by placing a graphite gasket on both sides of the membrane. The device was covered by heating tapes and heated to the desired temperature. A thermocouple mounted beneath the disk was used to control the temperature. High-purity hydrogen and nitrogen were used in all experiments. All the gases were fed to the permeator using calibrated mass-flow controllers. The Pd alloy side of the membrane was in contact with feed gases, while the other side was contacted with N_2 as a sweep gas (permeate side) during the heating procedure. No sweep gas was used on the permeate side during the single-gas permeation experiments. Pressure differences across the membranes were controlled using a back-pressure regulator. The upstream pressure was varied while keeping the downstream pressure constant at 100 kPa. The gas permeation flow rates of either H_2 or N_2 were measured using two bubble flow meters at room temperature and pressure. The permeation areas were 1.2 cm^2. All temperature changes were carried out in N_2 atmosphere.

To evaluate their responses to H_2S, initially all the membranes were exposed to a 100 ppm H_2S/H_2 gas mixture at 673 K for 24 h at a trans-membrane pressure of 50 kPa. After the H_2S exposure, pure hydrogen was fed into the system at the same temperature and pressure in order to evaluate the flux recovery.

(i) *Effect of temperature on the hydrogen regeneration:* After the H_2S exposure and H_2 treatment at 673 K, membranes were heated to 773 K (in H_2) for 24 h. After the 500 °C treatment, the samples were cooled to 673 K and the hydrogen flux was measured.
(ii) *Effect of temperature on H_2S corrosion:* To assess the effect of the temperature of H_2S exposure on the permeation properties, after experiment (*i*), one membrane was exposed to a 100 ppm H_2S/H_2 stream at 773 K, followed by the hydrogen recovery experiment at the same temperature.
(iii) *H_2S cycling treatment:* For a preliminary evaluation of the response of the membrane over more than one H_2S exposure–H_2 recovery cycle, a second cycle was conducted using one membrane.

The hydrogen flux through the membrane was measured at all the stages in the membrane treatment. No sweep gas was fed on the permeate side during these experiments. Nitrogen transport across the membrane was not detected at a trans-membrane pressure of 100 kPa either before or after the H_2S treatments, showing that neither the thermal treatment nor the H_2S exposure had a detrimental effect on the selectivity.

2.4. H_2S exposure of alloy samples for XPS depth profiling

For the XPS depth profiling analysis, annealed samples of a PdCuAu coated PSSD sample were cut into four pieces and each quarter was treated at conditions that simulated those used in the permeation experiment:

(i) the first piece was analyzed without treatment;
(ii) the other pieces were mounted horizontally in a tube furnace and then, exposed to a 100 ppm H_2S/H_2 mixture at 673 K for 24 h;
(iii) after that, two of these pieces were treated in a H_2 flux at 673 K for 48 h;
(iv) then, one of these pieces was exposed to a H_2 stream at 773 K for 24 h.

After each treatment, the samples were analyzed by XPS-depth profiling.

3. Results and discussion

3.1. Hydrogen permeation properties

To study the hydrogen permeation properties and the effects of H_2S exposure on the PdCuAu alloys, several membranes with different compositions were synthesized by sequential electroless deposition. The alloy composition selections were guided by high-throughput studies of sulfur-uptake on CSAF combinatorial libraries conducted at Carnegie Mellon University. Preparation of $Pd_xCu_yAu_{100-x-y}$ CSAFs has been described previously [24]. Briefly, a $\sim$100 nm-thick PdCuAu alloy film was deposited onto a $14 \times 14 \times 2$ mm^3 Mo substrate using three e-beam evaporative sources. Rotatable shadow masks, located between each source and the substrate, created a flux gradient of each component across the substrate surface to deliver a film with continuously varying composition that covered the entire composition space (x=0→100 and y=0→100−x). The as-deposited CSAF was annealed in vacuum for 1 h at 796 K. The annealed film was exposed to 100 ppm H_2/H_2S at 673 K for 24 h. Fig. 1 shows the

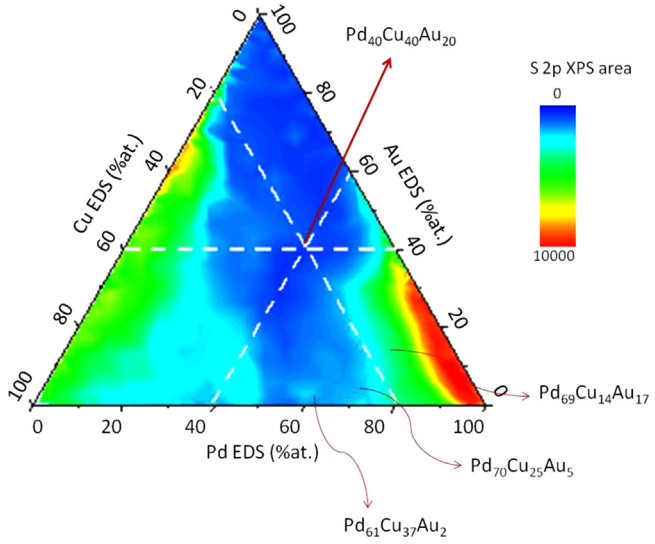

Fig. 1. Relative S-content of the CSAF's surface as a function of alloy composition, measured as relative S2p XPS signal. Treatment: 100 ppm H_2S/H_2, 673 K, 24 h.

sulfur-content of the CSAF's surface as a function of alloy composition, measured as S2p XPS signal. Sulfur-uptake is lowest, and the potential for resistance to S-corrosion is greatest, at compositions near $Pd_{40}Cu_{20}Au_{40}$. Alloy compositions used in the present work are indicated in the figure; they were chosen from regions that displayed relatively low S uptake, but with Pd contents higher than in $Pd_{40}Cu_{20}Au_{40}$ to maximize H_2 permeability.

The hydrogen permeation behavior of the $Pd_{60}Cu_{37}Au_3$, $Pd_{70}Cu_{25}Au_5$, $Pd_{69}Cu_{14}Au_{17}$ membranes, each annealed at 773 K in pure hydrogen for 5 days to ensure complete alloy formation [23], was studied as a function of temperature, with H_2 pressure differences between 10 and 100 kPa. Fig. 2 shows the hydrogen permeation flux through the $Pd_{69}Cu_{14}Au_{17}$ membrane as a function of $\Delta(P^{0.5}) = (P_{ret}^{0.5} - P_{perm}^{0.5})$ at 400 and 723 K. The hydrogen permeation flux displayed a linear dependence on the square root of the H_2 partial pressure at both temperatures, consistent with the solution-diffusion mechanism of hydrogen transport through a palladium-based membrane, where the rate-determining step is the diffusion of H in the metallic alloy bulk film. The other membranes exhibited the same linear relationship between flux and $\Delta(P^{0.5})$.

Fig. 3 compares the H_2 permeation fluxes at 723 K for the PdCuAu ternary alloy membranes to those of Pd, $Pd_{67}Cu_{33}$ and $Pd_{91}Au_9$ membranes prepared in our lab by electroless deposition. In all experiments, no nitrogen permeation was detected up to 723 K and 100 kPa, which implies that the membranes were defect-free. While none of the alloy membranes display permeabilities as high as pure Pd, both $Pd_{91}Au_9$ and $Pd_{69}Cu_{14}Au_{17}$—the ternary with the highest Au content—have permeabilities approaching that of pure Pd. Note also that among the three alloys with Pd ~70%, $Pd_{67}Cu_{33}$, $Pd_{70}Cu_{25}Au_5$ and $Pd_{69}Cu_{14}Au_{17}$, substitution of Au atoms for Cu atoms significantly increases permeability.

Table 2 compares the hydrogen permeabilities of the membranes from Fig. 3 to those from other relevant literature reports at 673 K and $\Delta P = 50$ kPa. Coulter et al. [21] reported experimental and predicted hydrogen permeabilities for several PdCuAu ternary alloy membranes. The authors presented a set of results from PdCuAu samples with different atomic compositions (Cu content 9–41 at% and Au content 4–9 at%) synthesized by magnetron sputtering [21]. Consistent with our results, they report an increase in hydrogen permeability with the substitution of Au for Cu: $Pd_{72}Cu_{26}Au_2$ and $Pd_{72}Cu_{20}Au_8$ alloys displayed

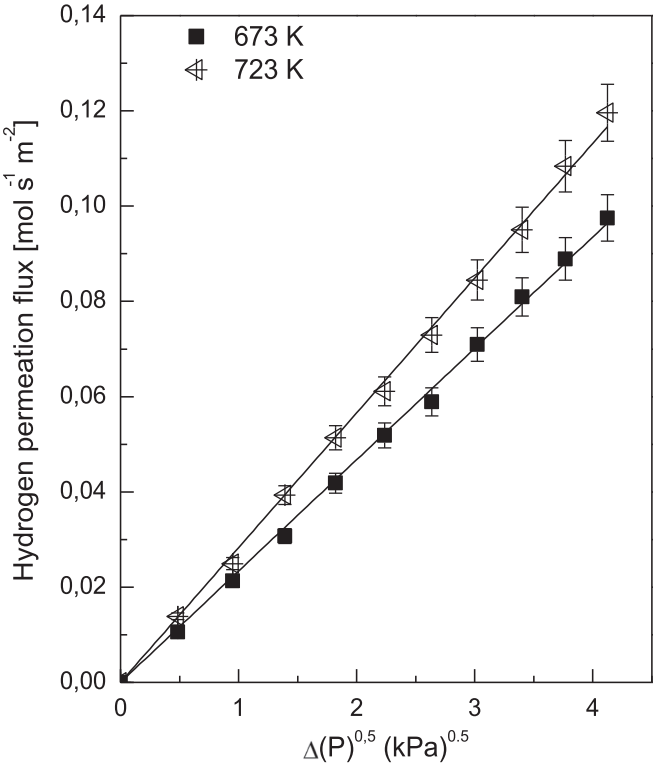

Fig. 2. Hydrgen permeation flux at 673 K and 723 K as a function of pressure gradient for the $Pd_{69}Cu_{14}Au_{17}$ membrane before H_2S exposure.

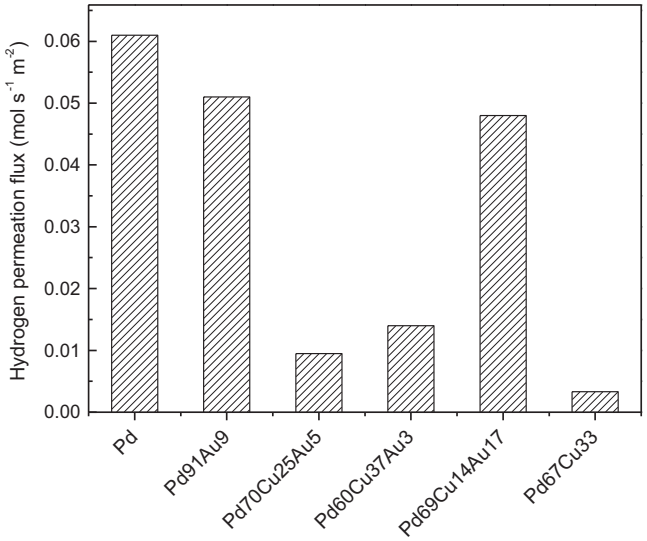

Fig. 3. Hydrogen permeation flux at 673 K and 50 kPa for the PdCuAu membranes before H_2S exposure.

permeabilities of 3×10^{-9} and 6.3×10^{-9} mol s^{-1} m^{-1} $Pa^{-0.5}$, respectively, at 400 °C. Peters et al. [17] compared the hydrogen permeability of several PdCuM ternary alloy membranes synthesized by magnetron sputtering to those of $Pd_{70}Cu_{30}$ binary alloys. A slight increase in permeability compared with the $Pd_{70}Cu_{30}$ binary alloy was reported for the PdCuAu system with a composition of about $Pd_{71.5}Cu_{27}Au_{1.5}$ (4.2×10^{-9} mol s^{-1} m^{-1} $Pa^{-0.5}$) when the sample was exposed to a 90% H_2/N_2 mixture using Ar as sweep gas.

Table 2
Hydrogen permeabilities of the PdCuAu membranes in pure hydrogen compared with literature data.

Sample	Thickness [μm]	Permeability [mol s^{-1} m^{-1} $Pa^{-0.5}$]	Permeability relative to pure Pd	Reference
$Pd_{70}Cu_{25}Au_5$	14	1.9×10^{-9} [a]	0.16	This work
$Pd_{60}Cu_{37}Au_3$	14	2.9×10^{-9}[a]	0.24	This work
$Pd_{69}Cu_{14}Au_{17}$	14	8.7×10^{-9}[a]	0.73	This work
$Pd_{91}Au_9$	12	9.9×10^{-9}[a]	0.82	[18]
$Pd_{67}Cu_{33}$	26	1.3×10^{-9}[a]	0.10	[27]
Pd	14	1.2×10^{-8}[a]	1	[18]
$Pd_{72}Cu_{26}Au_2$	10	3.0×10^{-9} [b]	0.27	[21]
$Pd_{72}Cu_{20}Au_8$	10	6.3×10^{-9} [b]	0.56	[21]
$Pd_{56}Cu_{41}Au_3$	10	1.5×10^{-9} [b]	0.13	[21]
$Pd_{83}Cu_{10}Au_7$	10	9.0×10^{-9} [b]	0.81	[21]
$Pd_{71.5}Cu_{27}Au_{1.5}$	2.1	4.2×10^{-9} [c]	0.42	[17]
$Pd_{72.1}Cu_{24.7}Au_{3.2}$	2.1	3.8×10^{-9} [c]	0.38	[17]

[a] Before H_2S exposure, temperature = 673 K , ΔP = 50 kPa.
[b] Data reported at 673 K
[c] Feed: 90% H_2/N_2, Ar sweep gas, temperature = 673 K

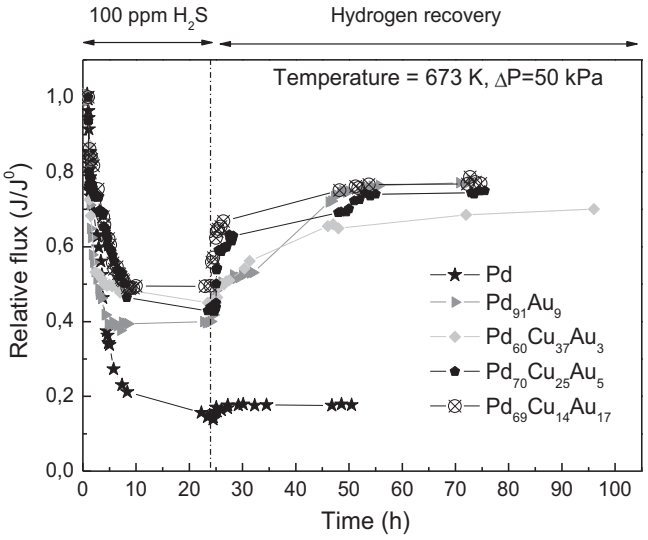

Fig. 4. Relative hydrogen flux (J/J^0) during the H_2S treatment at 673 K and subsequent flux recovery through the PdCuAu membranes as a function of time.

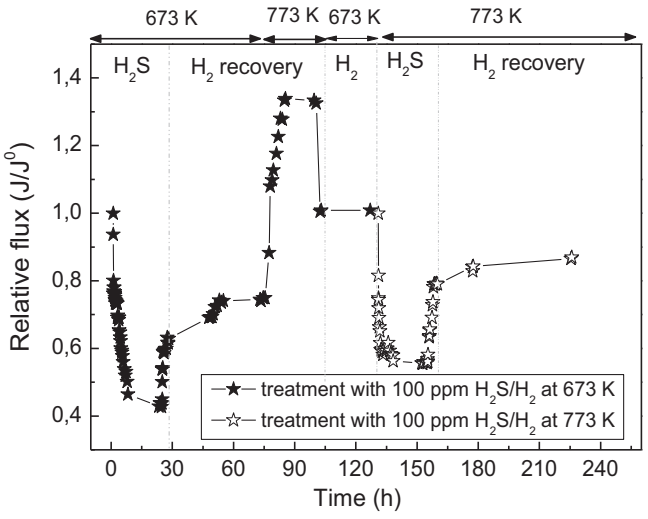

Fig. 5. Relative hydrogen flux (J/J^0) during the 100 ppm H_2S/H_2 treatment and subsequent flux recovery for the $Pd_{70}Cu_{25}Au_5$ membrane.

3.2. Effect of H_2S in membrane performance and flux recovery after treatment

To study the effect of H_2S on the hydrogen permeability of the PdCuAu ternary alloy membranes, a stream of 100 ppm H_2S/H_2 was introduced into the reactor at 673 K at the end of the pure H_2 gas permeation test. After 24 h of H_2S treatment, the gas feed was changed back to pure hydrogen to examine the flux recovery at 673 K. Fig. 4 shows the relative flux (J/J^0 where J is the H_2 flux at a given time and J^0 is the initial H_2 flux measured in pure H_2 at 673 K) as a function of time during H_2S exposure and then during subsequent recovery in H_2 at 673 K for the $Pd_{70}Cu_{25}Au_5$, $Pd_{69}Cu_{14}Au_{17}$ and $Pd_{60}Cu_{37}Au_3$ ternary membranes; results for Pd and $Pd_{91}Au_9$ samples are included for comparison. For all samples, the flux drops immediately upon introduction of H_2S. After 24 h in H_2S, the ternary membranes' H_2 fluxes have decreased by ~50–57%; the PdAu binary by ~60%; and Pd by 85%. As previously reported, the primary cause of the initial rapid decline is site blocking by adsorbed H_2S [10], while a slower continuous decrease, as observed for Pd, suggests bulk sulfidation

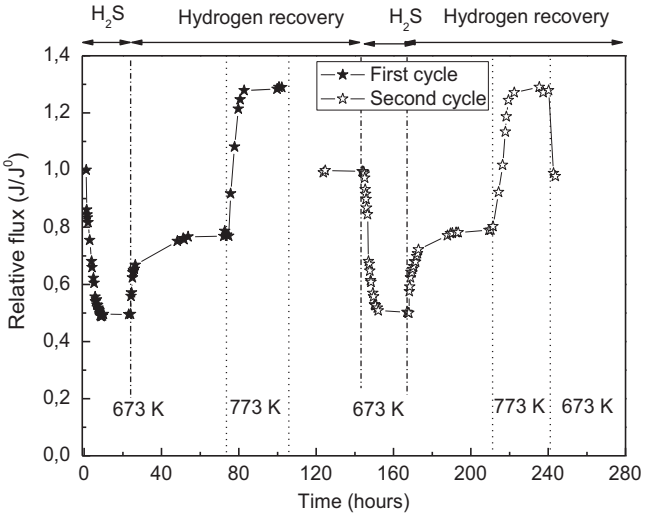

Fig. 6. Relative hydrogen flux (J/J^0) during the 100 ppm H_2S/H_2 treatment and subsequent flux recovery for the $Pd_{69}Cu_{14}Au_{17}$ membrane.

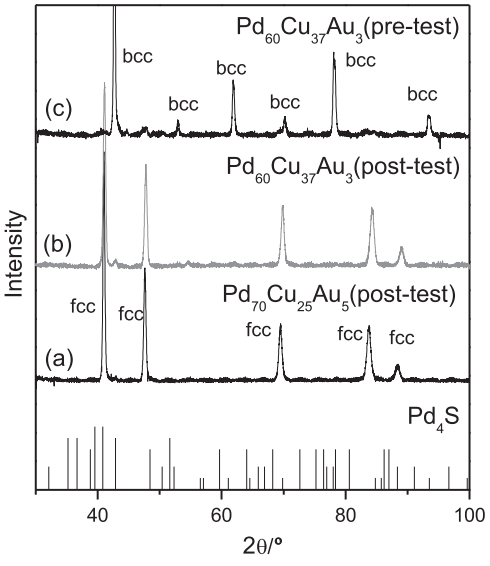

Fig. 7. XRD patterns of the PdCuAu membranes: (a, b) after H_2S exposure and subsequent hydrogen recovery treatment (post-test); and (c) before H_2S exposure (pre-test). The bars correspond to the Pd_4S phase.

[10]. The Pd membrane exhibited only a minor flux recovery upon H_2S removal, again consistent with formation of a bulk sulfide. In contrast, the PdCuAu ternary membranes displayed a fast partial recovery of H_2 permeability, likely related to reductive desorption of sulfur that had been blocking surface sites. After the first recovery stage, the alloy samples exhibited additional, but slower recovery that stabilized after about 50 h. However, none of the alloys recovered all of their original pure H_2 permeability at 673 K. The recovered flux for the $Pd_{70}Cu_{25}Au_5$ and $Pd_{69}Cu_{14}Au_{17}$ membranes was about 75% of the original value at 673 K, similar to the recovery of $Pd_{91}Au_9$. At 70%, $Pd_{60}Cu_{37}Au_3$ membrane recovered slightly less of its lost flux than the other alloys. Complete recovery at 673 K is likely prevented by strongly adsorbed S and/or formation of thin two-dimensional sulfide layers, as previously reported for other systems [10,18]. The ideal H_2/N_2 selectivity of the ternary alloy membranes remained unchanged after H_2S treatment followed by hydrogen recovery, suggesting that the exposure/recovery process did not impair the structural integrity of the membranes.

To study the effect of temperature on the H_2 recovery, after the H_2 recovery at 673 K, the $Pd_{70}Cu_{25}Au_5$ membrane was heated to 773 K in H_2 for another 24 h. Fig. 5 shows the relative hydrogen

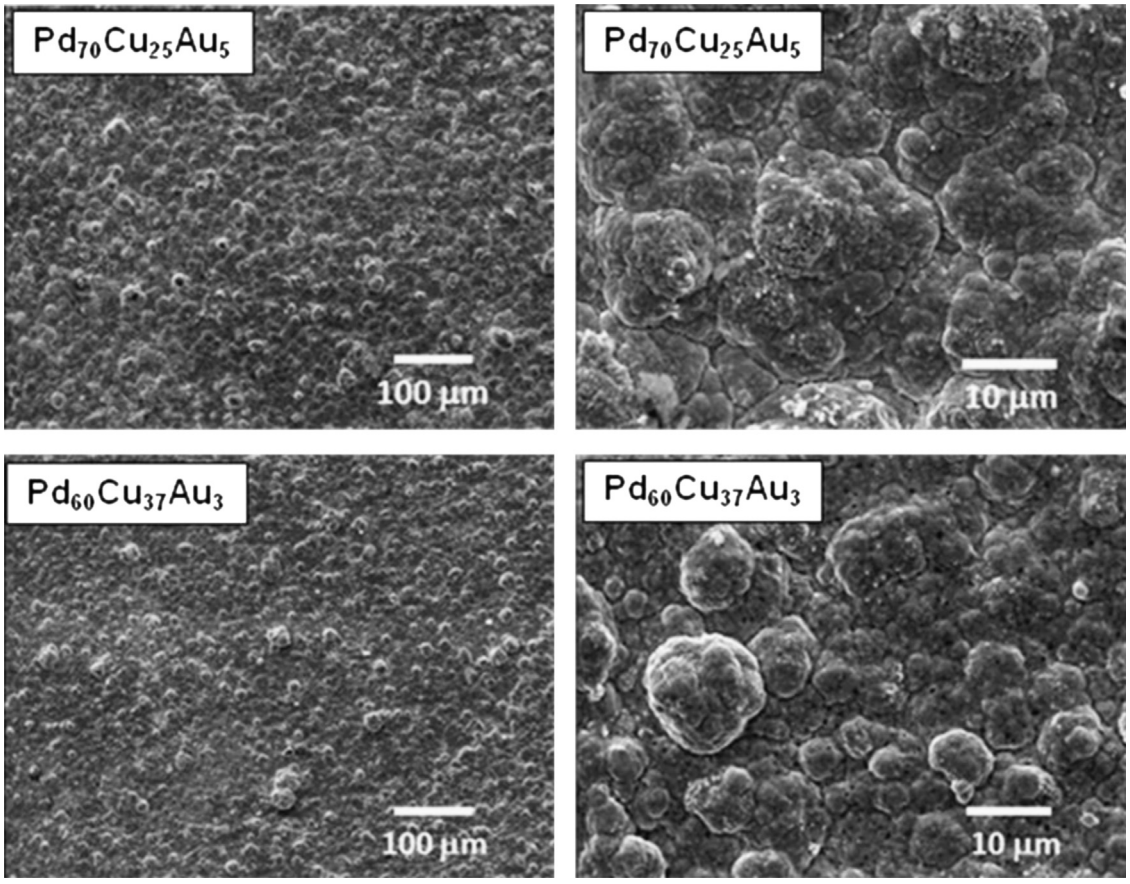

Fig. 8. SEM top view of the $Pd_{70}Cu_{25}Au_5$ and the $Pd_{60}Cu_{37}Au_3$ membranes after H_2S exposure and subsequent hydrogen recovery treatment.

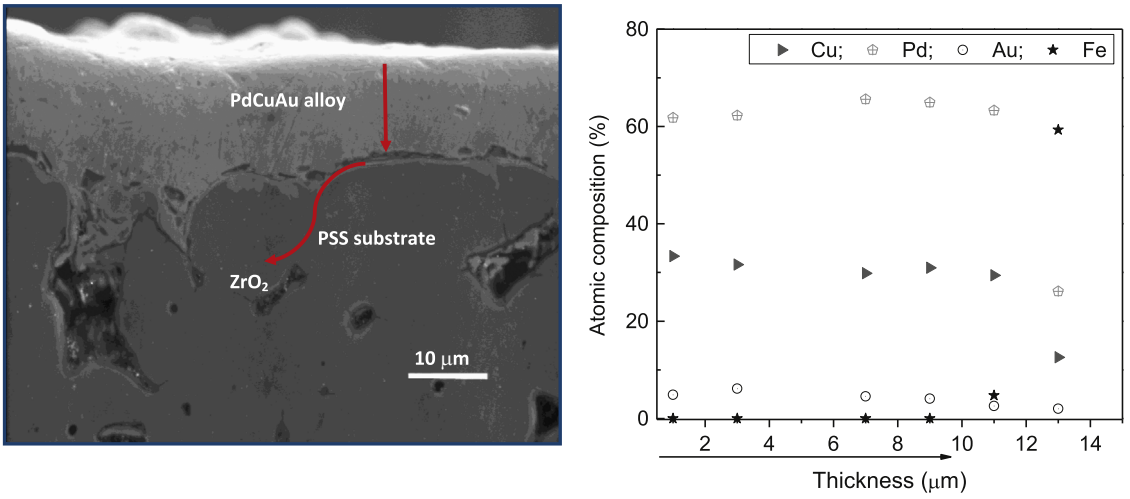

Fig. 9. SEM cross-section view and EDS measurements along the line through the $Pd_{60}Cu_{37}Au_3$ membrane.

flux for this sample as a function of the time on stream. Upon heating to 773 K, the hydrogen flux increased for about 7 h before reaching a new steady state. After 24 h at 773 K, the sample was cooled back to 673 K, where the H_2 flux was the same as it was at the beginning of the experiment—in other words, the membrane had fully recovered from the 673 K H_2S exposure. This pattern of recovery can be explained by considering two types of S adsorbed on the surface of the alloys: a weakly adsorbed S, which can be removed at 673 K and a strongly adsorbed sulfur/surface sulfide, which needs a higher temperature to be removed (773 K). Consistent with our results, Chen and Ma [10] reported nearly complete recovery of 673 K permeability, upon H_2 treatment of an H_2S-exposed $Pd_{95}Au_5$ membrane at 773 K. They suggested that because the dissociative adsorption of H_2S on a metal surface is exothermic, reductive desorption of adsorbed sulfur becomes more favorable at higher temperatures due to the shifting of equilibrium toward gas phase [10]. Furthermore, temperature would also influence the kinetics of the reductive desorption process and so, further studies are needed to understand the effect of temperature on the hydrogen recovery of Pd-based alloys.

After the 773 K flux recovery experiment, $Pd_{70}Cu_{25}Au_5$ was exposed to a 100 ppm H_2S/H_2 stream at 773 K to evaluate the effect of temperature on H_2S poisoning (starting at about 130 h in Fig. 5). As was the case at 673 K, introduction of H_2S at 773 K caused a significant and rapid decline in H_2 flux. After 24 h in the H_2S/H_2 stream, the flux had dropped to 45% of its pre-exposure value at 773 K, less than the 56% loss was observed at 673 K. Upon removal of H_2S (still at 773 K), the sample recovered 86% of its original flux, higher than the recovery of 74% observed at 673 K. This difference can be explained by exothermic nature of the dissociative adsorption of H_2S on metals, as described above. Consistent with our results, Way et al. recently reported a lower flux inhibition and greater flux recovery at higher temperature (773 K) for a $Pd_{74}Au_{12}Ag_{14}$ membrane exposed to 20 ppm H_2S in H_2 [20]. For a PdAu membrane, Chen and Ma [10] reported a 97% hydrogen recovery after 54.8 ppm H_2S exposure at 773 K for 4 h. The time required to obtain this recovery was about 70 h. In the same work, the authors stated that longer H_2S exposure times increased the time required to recover the steady-state flux. While for an exposure time of 4 h at 673 K the membrane reaches a steady-state after about 70 h, for an H_2S exposure time of 24 h, this value was reached after 180 h in a hydrogen stream.

Fig. 6 displays results of two full cycles of (1) H_2S exposure at 673 K, (2) recovery in H_2 at 673 K, and (3) recovery at 773 K for $Pd_{69}Cu_{14}Au_{17}$. As was the case for the $Pd_{70}Cu_{25}Au_5$ sample, a complete hydrogen recovery after H_2 treatment at 773 K was observed. Membrane response in the second cycle was similar to that in the first cycle, with 99% flux recovery after the second 773 K H_2 treatment. Both the $Pd_{70}Cu_{25}Au_5$ and $Pd_{69}Cu_{14}Au_{17}$ membranes were stable after a total of 550 h, including the annealing at 773 K, the pure hydrogen permeation measurements, and the H_2S-hydrogen recovery cycles.

XRD patterns of $Pd_{70}Cu_{25}Au_5$ and $Pd_{60}Cu_{37}Au_3$ membranes that were exposed to H_2S and then recovered in H_2 at 673 K are shown in

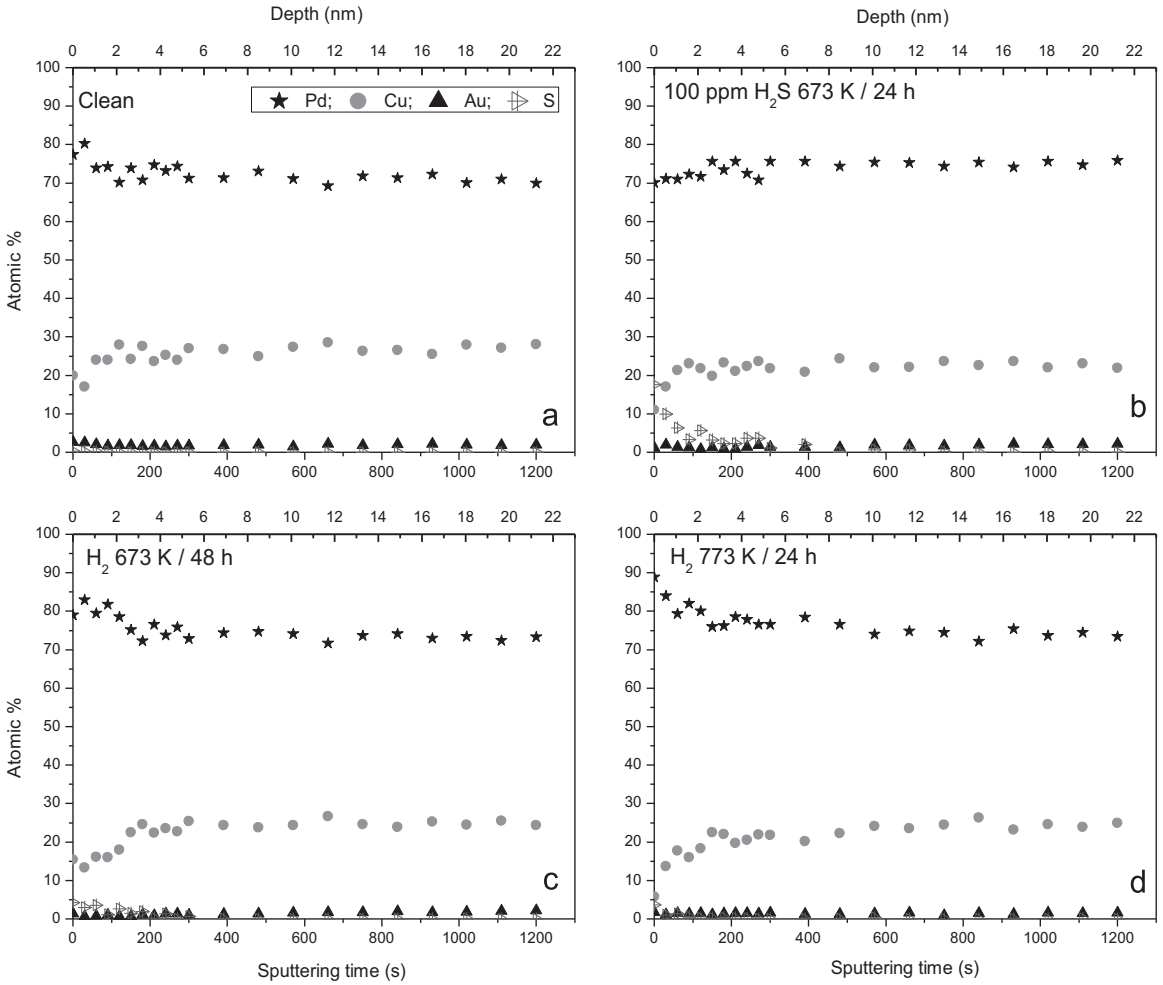

Fig. 10. XPS-depth profiles of the $Pd_{71}Cu_{26}Au_3$: (a) clean sample; (b) after 24 h of exposure at 100 ppm H_2S/H_2 at 673 K, (c) after H_2 recovery at 673 K 48 h and (d) after H_2 recovery at 773 K 24 h. Analysis conditions: 1st 10 steps of 30 s each. 2nd 10 cycles of 90 s each.

Fig. 7a and b. These patterns contain only features that can be indexed to the fcc structure of the parent alloy; there is no evidence of formation of bulk sulfides (for reference, the locations of features for Pd_4S are shown at the bottom of Fig. 7). The XRD pattern of $Pd_{70}Cu_{25}Au_5$ is characteristic of a fcc alloy structure, which is expected for that composition. The pattern of $Pd_{60}Cu_{37}Au_3$ is dominated by fcc features, but also contains smaller peaks that are indexed to a bcc alloy structure. This is an interesting result because the equilibrium structure of $Pd_{60}Cu_{37}Au_3$, shown in Fig. 7c for $Pd_{60}Cu_{37}Au_3$ that had been annealed in H_2 for 5 days (without H_2S exposure) at 773 K, is exclusively bcc. Probably, at 773 K the system is close to the fcc/bcc phase boundary and some aspect of the H_2S exposure and recovery sequence destabilizes the bcc form.

Fig. 8 shows the SEM top views of the $Pd_{70}Cu_{25}Au_5$ and $Pd_{60}Cu_{37}Au_3$ membranes after H_2S exposure followed by H_2 recovery treatment at 673 K. Both samples present a uniform morphology, with no evidence of cracks or pinholes. In agreement with the XRD analysis, sulfur was not detected by EDS in either sample, indicating that sulfur poisoning of the PdCuAu alloys during H_2S exposure occurs at or near the top surface of the membrane. To evaluate variations in membrane composition across the thickness of the membrane, the $Pd_{60}Cu_{37}Au_3$ sample was characterized by cross-section SEM–EDS. Fig. 9 shows the SEM cross section image and the EDS composition depth profile of the sample after the 100 ppm H_2S/H_2 permeation measurement followed by hydrogen recovery treatment at 673 K. The EDS results revealed a homogeneous Pd, Cu and Au composition across the film thickness. Note that no sulfur was detected, even near the surface of the sample, which is in agreement with the XRD data (Fig. 7).

3.3. XPS depth-profile characterization before and after H_2S exposure

To evaluate composition changes at the top surface (~40 nm) of the PdCuAu ternary alloys, both after exposure at 100 ppm H_2S/H_2 at 673 K and after the hydrogen recovery treatment, XPS-depth profile experiments were performed. Two ternary alloy samples, $Pd_{71}Cu_{26}Au_3$ and $Pd_{61}Cu_{37}Au_2$, were cut into four pieces and each quarter was treated as follows: (1) the first piece was evaluated without treatment; the other pieces were exposed to a 100 ppm H_2S/H_2 stream at 673 K for 24 h; (2) two of these pieces were treated in H_2 at 673 K for 48 h to allow characterization of the surface after the hydrogen recovery and, (3) one of these quarters was exposed to a hydrogen stream at 773 K for 24 h. After the treatments, the samples were analyzed by XPS-depth profile and SEM–EDS.

Fig. 10 shows the atomic surface composition of Pd, Cu, Au and S as a function of depth for the $Pd_{71}Cu_{26}Au_3$ alloy after each treatment described above. The depth profile of the as prepared sample (Fig. 10a) showed Pd-enrichment within the first ~10 nm of the alloy's top surface. Below 10 nm, the concentrations of Pd, Cu and Au reached steady state values that were the same as the bulk composition determined by EDS. After H_2S exposure, sulfur had penetrated ~10 nm into the sample with a maximum atomic concentration of ~15% at the top surface. Concurrently, the Pd concentration in the top 10 nm decreased, suggesting that S atoms replaced Pd atoms in

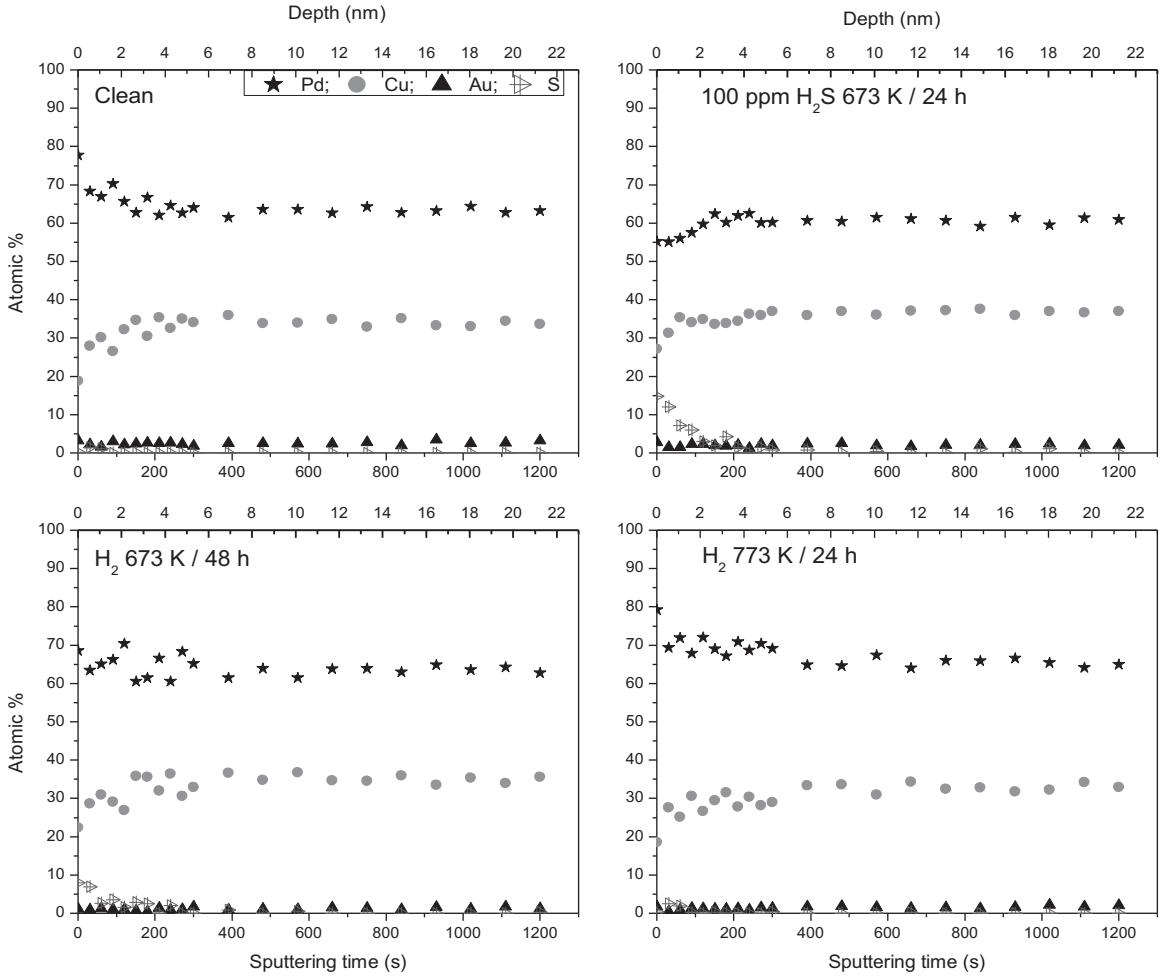

Fig. 11. XPS-depth profiles of the $Pd_{61}Cu_{37}Au_2$: (a) clean sample; (b) after 24 h of exposure at 100 ppm H_2S/H_2 at 673 K, (c) after H_2 recovery at 673 K 48 h and (d) after H_2 recovery at 773 K 24 h. Analysis conditions: 1st 10 steps of 30 s each. 2nd 10 cycles of 90 s each.

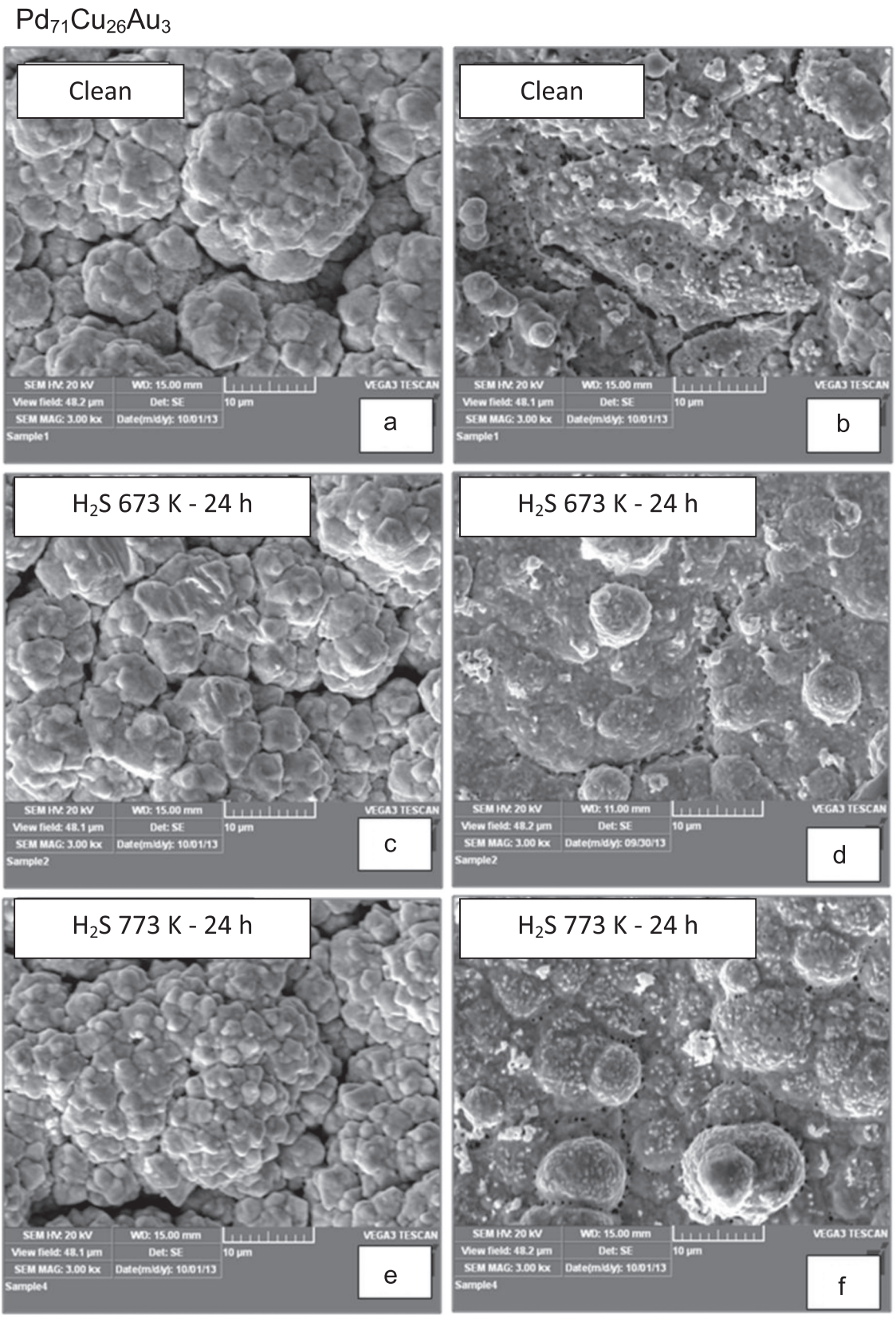

Fig. 12. SEM top view of the $Pd_{71}Cu_{26}Au_3$ (a, c, e) and $Pd_{61}Cu_{37}Au_2$ (b, d, f) membranes: (a, b) clean samples; (c, d) after H_2S exposure followed by a hydrogen stage at 673 K; and (e, f) after hydrogen treatment at 773 K.

that region during H_2S exposure. When a hydrogen recovery treatment at 673 K for 48 h was performed, the sulfur content of the top 10 nm decreased significantly, leaving a maximum atomic sulfur concentration of ~5% remaining at the top surface. A subsequent hydrogen treatment at 773 K produced a further decrease in the sulfur content of the sample to 3%, and no S was observed beyond ~2 nm into the sample. Similar depth profile patterns were observed for the $Pd_{61}Cu_{37}Au_2$ sample (Fig. 11), but the S atomic concentration after the

hydrogen recovery stage at 673 K, ~10%, was slightly higher than for the $Pd_{71}Cu_{26}Au_3$ sample. The patterns observed in S-depth profiles parallel those of the flux measurements. The correspondence between S content and flux suggests that the suppressed flux observed after hydrogen treatment at 673 K is related to formation of a shallow sulfur-containing near surface region, which extends only ~10 nm into the sample. The state of the surface can be thought of as strongly bound surface S atoms or, perhaps a two-dimensional surface sulfide. Unlike Pd, it is clear that PdCuAu does not form a thick bulk sulfide. High temperature (773 K) H_2 treatment of the H_2S exposed ternary alloy can reduce the surface sulfide and return the alloy to its original permeability.

Top-surface SEM micrographs of the $Pd_{71}Cu_{26}Au_3$ and $Pd_{61}Cu_{37}Au_2$ alloys after each treatment are shown in Fig. 12. Note that none of the PdCuAu alloys exhibited a significant morphological change upon exposure to 100 ppm H_2S/H_2 at 673 K (Fig. 11c). EDS analysis after treatment at 773 K in hydrogen did not revealed the presence of S in either sample, in agreement with XRD results.

We also note that, while Pd enrichment of the surface region was observed in the depth profile of the as prepared PdCuAu alloy, top-surface compositions measured by LEIS suggest Cu enrichment at the top-most atomic layer as we previously reported [23]. The presence of excess Cu atoms at the top surface, where H_2S first interacts with the alloy, may contribute to the alloy's resistance to corrosion beyond the 10 nm surface region.

4. Conclusions

PdCuAu ternary alloy membranes with different atomic composition were synthesized by sequential electroless deposition on top of porous stainless steel supports. The ternary membrane with the highest Au content, $Pd_{69}Cu_{14}Au_{17}$, exhibited the highest hydrogen permeation flux, similar to that of a $Pd_{91}Au_9$ membrane.

Upon exposure to 100 ppm H_2S/H_2 at 673 K for 24 h, the PdCuAu membranes experienced significant flux reductions of about 55%, followed by recovery to ~80% of the initial hydrogen flux upon treatment in pure H_2 at 673 K. The permeance loss and flux recovery were temperature dependent with a lower decrease and higher recovery at higher temperature as corroborated through the $Pd_{70}Cu_{25}Au_5$ membrane. For the complete hydrogen recovery flux after H_2S exposure, a treatment at a higher temperature was needed. After exposure to 100 ppm, H_2S/H_2 the membranes displayed a fcc diffraction pattern with no evidence of bulk sulfide formation. In agreement with XRD and SEM results, sulfur was not detected in the bulk of PdCuAu ternary alloy samples by EDS.

The XPS-depth profiles of the $Pd_{61}Cu_{37}Au_2$ and $Pd_{71}Cu_{26}Au_3$ samples show low sulfur content on the top-surface after H_2S exposure, which disappears about 10 nm into the bulk. The depth profiles of the samples after the hydrogen recovery treatment at 673 K for 48 h, followed by treatment at 773 K for 24 h, show very low sulfur content (~3%), in agreement with the hydrogen flux recovery observed through the $Pd_{70}Cu_{25}Au_5$ membrane.

The data presented in this work suggest that the PdCuAu alloys are promising materials to be applied as membranes for hydrogen purification and exhibit high resistance to H_2S contamination. However, further studies are needed to achieve both high permeability and high chemical resistant membranes.

Acknowledgments

The authors wish to acknowledge the financial support received from UNL (CAID 2012 PJ50020110100052LI), ANPCyT (PIP 2012-00955) and the NSF-CONICET Program (Grant 2011-2013). Thanks are given to Elsa Grimaldi for the English language editing. The authors also wish to acknowledge the National Science Foundation for its support of research on Pd-alloys for hydrogen separation at Carnegie Mellon (CBET 1033804).

References

[1] P. Ferreira-Aparicio, M. Benito, S. Menad, Catalysis in membrane reformers: a high-performance catalytic system for hydrogen production from methane, J. Catal. 231 (2005) 331–343.
[2] M.E. Ayturk, N.K. Kazantzis, Y.H. Ma, Modeling and performance assessment of Pd and Pd/Au-based catalytic membrane reactors for hydrogen production, Energy Environ. Sci. 2 (2009) 430–438.
[3] P. Pinacci, M. Broglia, C. Valli, G. capannelli, A. Comite, Evaluation of the water gas shift reaction in a palladium membrane reactor, Catal. Today 156 (2010) 165–172.
[4] J. Okazaki, D.A.P. Tanaka, M.A.L. Tanco, Y. Wakui, F. Mizukami, T.M. Suzuku, Hydrogen permeability study of the thin Pd–Ag alloy membranes in the temperature range across the alpha-beta phase transition, J. Membr. Sci. 282 (2006) 207–218.
[5] W.M. Tucho, H.J. Venvik, M. Stange, J.C. Walmsley, R. Holmestad, R. Bredesen, Effects of thermal activation on hydrogen permeation properties of thin, self-supported Pd/Ag membranes, Sep. Purif. Technol. 68 (2009) 403–410.
[6] C.P. O´Brien, B.H. Howard, J.B. Miller, B.D. Morreale, A.J. Gellman, Inhibition of hydrogen transport through Pd and $Pd_{47}Cu_{53}$ membranes by H_2S at 350 °C, J. Membr. Sci. 349 (2010) 380–384.
[7] A. Li, W. Liang, R. Hughes, The effect of carbon monoxide and stream on the hydrogen permeability of a Pd/stainless steel membrane, J. Membr. Sci. 165 (2000) 135–141.
[8] Ø. Hatlevik, S.K. Gade, M.K. Keeling, P.M. Thoen, A.P. Davidson, J.D. Way, Palladium and palladium alloy membranes for hydrogen separation and production: history, fabrication strategies, and current performance, Sep. Purif. Technol. 73 (2010) 59–64.
[9] N. Pomerantz, Y.H. Ma, Effects of H_2S on the performance and long-term stability of Pd/Cu membranes, Ind. Eng. Chem. Res. 48 (2009) 4030–4039.
[10] Ch-H. Chen, Y.H. Ma, The effect of H_2S on the performance of Pd and Pd/Au composite membrane, J. Membr. Sci. 362 (2010) 535–544.
[11] E. Ozdogan, J. Wilcox, Investigation of H_2 and H_2S adsorption on niobium and copper-dopped palladium surfaces, J. Phys. Chem. B 114 (2010) 12851–12858.
[12] M.V. Mundschau, X. Xie, C.R. Evenson, A.F. Sammells, Dense inorganic membranes for production of hydrogen from methane and coal with carbon dioxide sequestration, Catal. Today 118 (2006) 12–23.
[13] B.D. Morreale, M.V. Ciocco, B.H. Howard, R.P. Killmeyer, A.V. Cugini, R.M. Enick, Effect of hydrogen-sulfide on the hydrogen permeance of palladium–copper alloys at elevated temperatures, J. Membr. Sci. 241 (2004) 219–224.
[14] D.L. McKinley, Metal alloy for hydrogen separation and purification, US Patent, 3350845, 1967.
[15] S.K. Gade, S.J. DeVoss, K.E. Coulter, S.N. Paglieri, G.O. Alptekin, J.D. Way, Palladium–gold membranes in mixed gas streams with hydrogen sulfide: effect of alloy content and fabrication technique, J. Membr. Sci. 378 (2011) 35–41.
[16] K.E. Coulter, J.D. Way, S.K. Gade, S. Chaudhari, G.O. Alptekin, S.J. DeVoss, Sulfur tolerant PdAu and PdAuPt alloy hydrogen separation membranes, J. Membr. Sci. 405–406 (2012) 11–19.
[17] T.A. Peters, T. Kaleta, M. Stange, R. Bredesen, Development of ternary Pd-Ag-TM alloy membranes with improved sulphur tolerance, J. Membr. Sci. 429 (2013) 448–458.
[18] F. Braun, A.M. Tarditi, J.B. Miller, L.M. Cornaglia, Pd-based binary and ternary alloy membranes: morphological and perm-selective characterization in the presence of H_2S, J. Membr. Sci. 450 (2014) 299–307.
[19] F. Braun, J.B. Miller, A.J. Gellman, A.M. Tarditi, B. Fleutot, P. Kondratyuk, L. M. Cornaglia, PdAgAu alloy with high resistance to corrosion by H_2S, Int. J. Hydrog. Energy 37 (2012) 18547–18555.
[20] A.E. Lewis, H. Zhao, H. Syed, C.A. Wolden, J.D. Way, PdAu and PdAuAg composite membranes for hydrogen separation from synthetic water-gas shift streams containing hydrogen sulfide, J. Membr. Sci. 465 (2014) 167–176.
[21] K.E. Coulter, J.D. Way, S.K. Gade, S. Chaudhari, D.S. Sholl, L. Semidey-Flecha, Predicting, fabricating and permeability testing of free-standing ternary palladium–copper–gold membranes for hydrogen separation, J. Phys. Chem. C 114 (2010) 17173–17180.
[22] T.A. Peters, T. Kaleta, M. Stange, R. Bredesen, Development of thin binary and ternary Pd-based alloy membranes for use in hydrogen production, J. Membr. Sci. 383 (2011) 124–134.
[23] A.M. Tarditi, C. Imhoff, J. Miller, L. Cornaglia, Surface properties of PdCuAu ternary alloys: a combined LEIS and XPS study, Surf. Interface Anal. (2015) (Submitted for publication).
[24] B. Fleutot, J.B. Miller, A.J. Gellman, Apparatus for deposition of composition spread alloy films: the rotatable shadow mask, J. Vac. Sci. Technol. A. 30 (2012) 061511–061521.
[25] Y.H. Ma, B.C. Akis, M.E. Ayturk, F. Guazzone, E.E. Enqwall, I.P. Mardilovich, Ind. Eng. Chem. Res. 43 (2004) 2936.
[26] A.M. Tarditi, C. Gerboni, L. Cornaglia, PdAu membranes supported on top of vacuum-assisted ZrO_2-modified porous stainless steel substrates, J. Membr. Sci. 369 (2011) 267–276.
[27] A.M. Tarditi, F. Braun, L.M. Cornaglia, Novel PdAgCu ternary alloy: hydrogen permeation and surface properties, Appl. Surf. Sci. 257 (2011) 6626–6635.